Dendrimer Nanodevices and Gallic Acid

Subjects: Nanoscience & Nanotechnology

Contributor: Silvana Alfei

Human neuroblastoma (NB), a pediatric tumor inclined to relapse, after an initial response to therapy, usually develops resistance. Since several chemotherapeutics, including the weel known etoposide (ETO), exert anticancer effect by increasing reactive oxygen species (ROS), NB cells overproduce antioxidant compounds becoming drugs-resistant. Moreover, ETO, although widely used, suffers from fast metabolism, poor solubility and systemic toxicity, that limit its administration dosage and its therapeutic efficiency. An appealing strategy to sensitize NB cells to chemotherapy involves the use of less toxic natural compounds able to reduce antioxidant defenses of NB cells and to induce ROS overproduction. In this contest, although affected by several issues as instability and poor absorbability, antioxidant/pro-oxidant polyphenols, such as gallic acid (GA), showed pro-oxidant anti-cancer effects and low toxicity for healthy cells, in several kind of tumors, not including NB. Herein, for the first time, free GA, two GA-dendrimers, and the dendrimer adopted as GA reservoir were tested on both sensitive and chemoresistant NB cells. Furthermore, the dendrimer adopted as carrier for GA was exploited also for entrapping and protecting ETO and for enhancing its solubility and effectiveness.The dendrimer device induced ROS-mediated death both in sensitive NB cells and also in chemoresistant ones. Free GA proved a dose-dependent ROS-mediated cytotoxicity on both cell populations. Intriguingly, when administered in dendrimer formulations at a dose not cytotoxic for NB cells, GA nullified any pro-oxidant activity of dendrimer. Unfortunately, due to GA, nanoformulations were inactive on NB cells, but GA resized in nanoparticles showed considerable ability in counteracting, at low dose, ROS production and oxidative stress, herein induced by the dendrimer. Interestingly, the ETO-dendrimer showed a synergistic action, controlled released over time with a significantly improved drug bioactivity, representing a novel biodegradable and promising device for the delivery of ETO into NB cells.

Keywords: Human neuroblastoma ; gallic acid (GA) ; polyester dendrimers ; dendrimer nanoformulations ; etoposide (ETO) ; ETO loaded dendrimer

1. Introduction

In the last decades, the correlation between oxidative stress (OS) and cancer onset has been highlighted by several pieces of evidence, but with contradictory findings. In fact, during the neoplastic transformation, there is an improvement in the production of reactive oxygen species (ROS), which supports tumor cell growth, by stimulating both redox-modulated signal transduction routes and transcription agents. In this regard, the use of ROS scavenging synthetic or natural compounds, counteracting the activation of redox sensitive pathways, could be employed as anti-carcinogenic for preventing the tumors onset and for treating the disease in the early stages.

When chemotherapeutic drugs induce an increase in intracellular ROS levels, the intrinsic antioxidant defense decreases and cancer cell death occurs. Therefore, in this perspective, antioxidants, contrasting the cytotoxic role of ROS, could favor neoplastic progression.

In this regard, an effective anti-tumor strategy could be to combine drugs capable of increasing ROS production with compounds able to reduce the intracellular antioxidant defenses. Human neuroblastoma (NB) is a solid tumor affecting young children, responsible for 15% of childhood cancer mortality [1][2][3].

NB is a heterogeneous tumor that origins from neural crest elements of the sympathetic nervous system and includes both low-risk forms, capable of regressing spontaneously or of differentiating into benign ganglioneuroblastoma, and high-risk (HR) forms, featured by metastatic disease and/or presence of MYCN proto-oncogene amplification. The amplification of MYCN is a biomarker still used today for early prognosticating risk and it is an indicative factor of poor prognosis [4].

Currently, HR patients undergo treatments, which include intensive and toxic chemotherapy followed by surgical resection, myeloablation and rescue of autologous stem cell, radiotherapy, and intensive immunotherapy [5].

Chemotherapeutic standard treatments consist of multi-drugs therapies, which combine several compounds including doxorubicin and etoposide (ETO). In particular, ETO is widely used [6][7][8] and induces a ROS-mediated anti-tumor effect. Unfortunately, its severe side effects [9][10] and chemoresistance limit its clinical success [11]. Moreover, poor water solubility, metabolic and non-metabolic inactivation, myelosuppression, and poor bioavailability are additional drawbacks related to ETO.

Chemoresistance is a multifactorial phenomenon and, recently, it has been demonstrated that ETO-resistant NB cells had high levels of glutathione (GSH) [12], which is the most important intracellular antioxidant thiol crucially involved in both cancer progression and chemoresistance [13]. In this context, the current trend of research, in the field of cancer treatment, increasingly focuses on developing alternative preventive and/or therapeutic strategies, based on the use of less toxic natural bioactive compounds, such as polyphenols, having both pro-oxidant and antioxidant activities, usually correlated to the dose [14].

Polyphenols, due to their antioxidant properties, have the possibility to act as preventive anti-cancer compounds [15], and, thanks to their pro-oxidant effects, they can work as mimics of chemotherapeutic drugs, inducing ROS-mediated cancer cell death [16].

It is the case of gallic acid (GA, Figure 1), which is the 3,4,5-*tri*-hydroxyls derivative of benzoic acid and represents one of the major phenolic acids present in various edible natural products, such as green tea, gallnuts, oak bark, apple peels, grapes, strawberries, pineapples, bananas, and many other fruits [17].

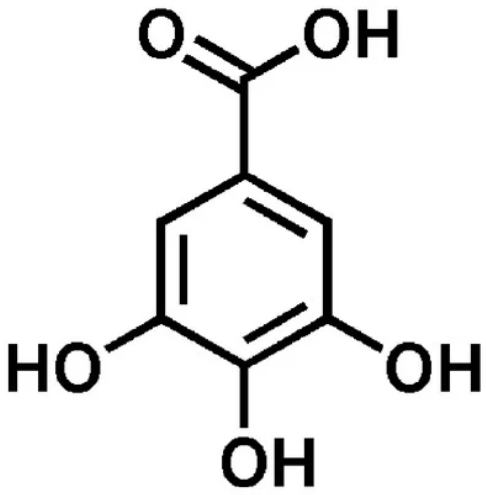

Gallic acid (GA) **1**

Figure 1. Chemical structure of gallic acid (GA) **1**.

The ingestion of these foods is justifiably correlated to beneficial outcomes for the human health, such as reduced risk of cardiovascular diseases and myocardial infarction, reduced predisposition to tumor diseases, and improvement of the quality of life in people suffering from neurodegenerative diseases or early stage tumors. Inside plants, GA is one of the secondary metabolites involved in the formation of the galatotannin-hydrolysable tannins, but, in the biomedical sector, it has long attracted the interest of scientists for its ambivalent antioxidant/pro-oxidant behavior [18] and its capacity in counteracting diseases correlated to OS, through its anti-bacterial, anti-viral, anti-inflammatory, anti-neurodegenerative, and anticancer activities [15][16][17][19][20][21][22][23][24][25][26][27][28][29].

Furthermore, GA finds applications in several other areas, including food and cosmetic industry, as natural preservative in food, beverages, beauty products, and essential oils, because of its free radicals scavenging activity (RSA) [30].

Several studies report that GA can counteract cancer growth and progression, thanks to its anti-invasive and anti-metastatic activities and that it could be useful both to treat neoplasia, inducing ROS production such as ETO, and to prevent malignant transformation, exerting a protective antioxidant effect on healthy cells [31][32][33][34].

Based on these findings and considering that, to our knowledge, no evidence proving significant GA activity against human NB cells has yet been reported yet, this compound, for the first time, was investigated as novel alternative therapeutic approach to treat this pediatric tumor. Unfortunately, GA is sparingly soluble in water and alcohols [35], practically insoluble in hydrophobic solvents, and its activity and clinical applications are hampered by additional drawbacks such as high instability and low bioavailability.

Luckily, the recent advances in the field of nanomedicine and in the use of nanoparticles (NPs), as convenient drug carrier systems capable of improving drug solubility, half-life, and bioavailability and of lessening the metabolism and systemic toxicity of several problematic bioactive compounds, including polyphenols, increasingly allow for further expansion of the possibilities of anticancer treatments by employing natural compounds.

In the last decades, dendrimers have arisen as the most talented NP carrier systems endowed with the possibility of revolutionizing cancer treatments. Dendrimers can be employed to efficiently deliver anti-neoplastic drugs and typically are used as scaffolding with a well-defined architecture or as nanovehicles to conjugate, complex, or entrap therapeutic drugs.

Structurally, dendrimers are symmetric monodisperse [36] tree-like macromolecules, with both internal cavities for guest molecule encapsulation [37] and several peripheral chemical groups for further functionalization by covalent bond.

Interestingly, they possess an unusually low intrinsic viscosity that makes easy their transport in the blood [38][39].

They possess the capability of controlling molecular weight, hydrophilicity, solubility [39][40][41], bioavailability, and pharmacokinetic behavior of transported drugs.

Thanks to dendrimer's ability in establishing strong interactions with several drugs, their loading results facilitated and their systemic toxicity, often due to the initial massive drug release (burst release), is minimized [39][40][41].

Among dendrimers, positively charged and commercially available poly(amidoamine) (PAMAMs) and polypropyleneimine (PPIs) are well-functioning for several biomedical applications, including gene therapy and drug delivery, but their clinical application is hampered by high non-selective cytotoxicity, hemolytic toxicity, genotoxicity, low biodegradability, fast removal from circulatory system, and high uptake in the reticuloendothelial system [42].

On the contrary, uncharged polyester dendrimer scaffolds appear more attractive and suitable for biomedical applications, because respectful of physiologic membranes and characterized by a good biodegradability [36][43][44].

Concerning ETO, inorganic nanohybrid constructs, consisting of layered double hydroxides (LDHs) intercalated with VP16 (ETO phosphate), have been successfully synthesized and characterized, that showed a high cytotoxic effect on cancer cells while being less toxic for healthy cells. However, although the results obtained from the employment of LDHs are promising, further improvements could be important in order to enhance some physicochemical properties, which are pivotal for a well-functioning nanosized drug delivery system, such as Z-potential and an increase in DL%. Among the strategies adopted, the use of dendrimer offers interesting perspectives . Concerning GA-enriched dendrimers, PAMAM dendrimers have been adopted both for covalently linking and for encapsulating GA [45][46], while PPI dendrimers have been used to solubilize GA and to control its release profile [47].

In addition, examples of biodegradable polyester-based dendrimers in which GA is either the repeated monomeric unity [48][49] or makes part of the dendrimer backbone [50] are reported.

In this work, thinking about a strategy to improve the outcomes from ETO treatments and about a future clinical application of GA, in order to ameliorate their solubility and stability, to slow down their metabolism, and to minimize the active dosage, a lab-made biodegradable dendrimer (namely, **4**) [51][52][53][54][55][56] was adopted for formulating both ETO and GA in NPs (Figure 2).

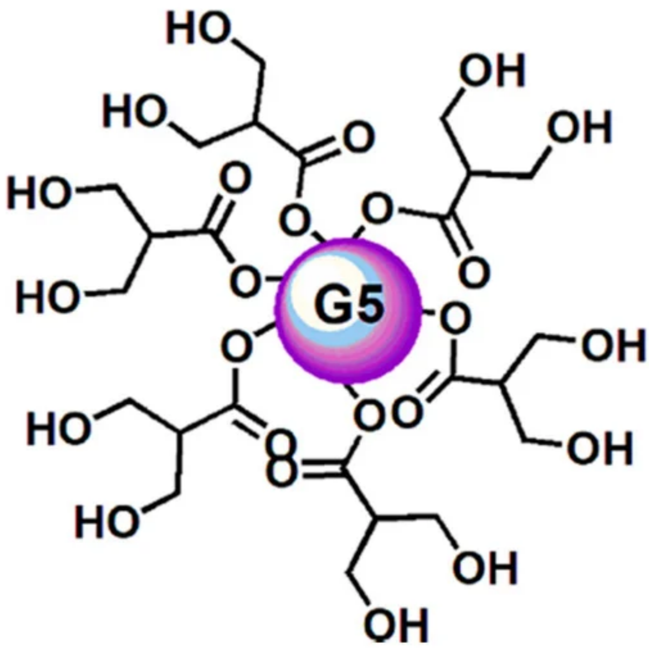

Figure 2. Simplified and intuitive representation of the structure of the dendrimer (**4**) having in reality a fifth-generation polyester-based inner matrix based on the tree-like repetition of units of the 2,2-*bis*(hydroxymethyl) propionic acid and 64 peripheral hydroxyl groups. The image shows only a partial number of the real hydroxyl groups and an inner sphere to facilitate the drawing and for reasons of space. This way to represent dendrimer **4** was previously used and accepted as valid [57].

Dendrimer **4** was selected for the serie of reasons following.

It has been reported [58] that the internal construction of a dendrimer, depending on its chemical structure, is suitable for complexing both hydrophobic and hydrophilic compounds [59].

Hence, in addition to being chosen for its intrinsic cytotoxic activity, the polyester-based dendrimer **4**, having hydrophilic characteristics, was considered suitable to host a hydrophilic molecule such as GA, with which it can establish hydrogen bonds.

In addition, being uncharged, it has been thought to also be well compatible with the phenyl hydrophobic portion of GA. Moreover, dendrimer **4** was considered a proper candidate carrier to entrap GA because, thanks to its high generation, it could offer more space to host drugs, thus allowing a higher loading [60].

Furthermore, the large chemical architectures, with wide surface and high molecular weight, achievable with high generation dendrimers such as **4**, characteristically remain in the blood circle for longer periods [61].

Finally, dendrimer **4** was preferred because its uncharged polyester-based hydrolysable architecture matches the requirements of low toxicity and high biodegradability desirable for biomedical applications [36][43][44].

Starting from these assumptions, dendrimer **4** was used for entrapping ETO in its inner cavities, thus proving ETO with a protective shell. The dendrimeric ETO-loaded NPs (ETOD) showed an highly improved solubility in hydrophilic and biocompatible solvents such as ethanol and water (by 37–390 times). Concerning GA, by using dendrimer **4**, firstly a GA-enriched dendrimer (GAD **6**, Figure 3a), in which GA is covalently linked on the dendrimer surface by ester type bonds, was synthetized according to a reported procedure [54].

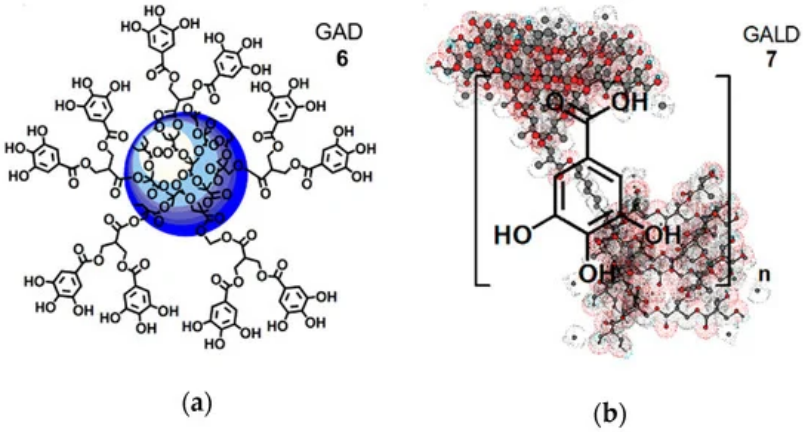

Figure 3. Simplified and intuitive representation of the GA-enriched dendrimers' structure: (**a**) structure of the GAD nanoconjugate (**6**); (**b**) structure of the GALD nanocomposite (**7**) encompassing the tri-dimensional representation of dendrimer **4** obtained by Chem3D Pro 7.0 software with included *n* molecules of GA. Concerning GAD, the blue sphere represents the inner polyester-based scaffold of dendrimer **4**; the five linkers, connecting two GA molecules each, are a stylized representation of the groups actually present on the surface of **4** that in reality possesses 32 analogous structures, for a total of 64 hydroxyl groups bearing 64 GA units.

Secondly, a GA-loaded dendrimer (GALD **7**, Figure 3b), in which GA is physically complexed with dendrimer **4**, through both inside entrapment and surface absorption, was prepared and totally characterized.

After investigations concerning the dose- and time-dependent GA effects on two NB cell lines differently sensitive to ETO [12][62], the biological activities of dendrimer **4**, free GA, and GA-enriched dendrimers **6** and **7** at specific selected doses were investigated as well.

2. Experimental

2.1. Materials

FTIR and NMR spectra of commercially available ETO are observable in Figure S3 accessible in Supplementary Materials (SM) accessible on line. Details concerning the characterization of commercial GA as copies of FTIR (lab-made) and ^{1}H and ^{13}C NMR spectra (database of Aldrich, Darmstad, Germany) are accessible in Section S3 (Figures S13–S15) in the SM available on line. Synthetized dendron intermediates (D4BnA, D4BnOH, D5BnA, and D5ACOOH) necessary to achieve dendrimer **4**, adopted as scaffold-carrier to link and entrap GA (**1**), were prepared according to what reported previously [51][52][53]. Their chemical structures are observable in Figure S1. Dendrimer **4** and GA-enriched dendrimer GAD **6** were prepared according to procedures previously reported [54][55][56].

Characterization data of dendrimer **4** and GAD **6**, counting copies of FTIR, ^{1}H and ^{13}C NMR spectra are accessible in SM (Section S1, Figures S3–S8, and Table S1). The protected/activated GA derivative (GA-TBDMS-Cl) necessary to esterify peripheral hydroxyls of dendrimer **4** was prepared reproducing the synthetic pathway shown in SM (Section S1, Scheme S1) [54]. Synthetic procedures for preparing ETOD and its detailed characterization data are accessible on line at https://doi.org/10.3390/antiox9010050.

2.2. Experimental procedure

Detailed experimental procedures are available in Section 2 of the original article available online at https://www.mdpi.com/2079-4991/10/6/1243/s1 and in Section 2 of the paper accessible on line at https://doi.org/10.3390/antiox9010050.

3. Results and Discussion

3.1. Preparation of ETO-Dendrimer Nanoformulation (ETOD)

A detailed discussion concerning the physicochemical properties of ETOD are accesible on line at https://doi.org/10.3390/antiox9010050, while a discussion on its bioactivity on sensitive NB cells (HTLA-230) is reported in the following sections of the present entry.

3.2. Preparation of GA-Dendrimer Nanoformulations GAD (6) and GALD (7)

Dendrimer NPs have proved to be particularly efficient in improving drugs therapeutic efficacy at lower dosages by behaving as “excipients” or enhancers of permeability, by altering the barrier properties of the intestinal epithelium, thus enhancing the permeation ability of the transported drug [61].

Following this current and successful trend, GA was previously formulated in NPs, by its covalent bond to a fifth-generation, biodegradable dendrimer matrix (**4**) obtaining a peripherally GA-decorated dendrimer (GAD), with appealing results from several points of view [54][55][56].

In the present study, GAD was prepared according to the above cited procedure , and, in addition, novel GA dendrimer NPs were achieved by physical complexation of GA with the architecture of dendrimer **4**. A drug delivery system of GA (GALD, **7**) was realized, in which, differently from GAD, GA units are not chemically linked on the surface, but are located inside the dendrimer matrix cavities or absorbed onto its surface, where they are withheld mainly by hydrogen bond interactions.

Concerning GAD, both the structure of dendrimer scaffold and of GA have been chemically modified by the mutual covalent bond. Differently, in GALD the structure of GA and dendrimer **4** were not modified during the synthetic pathway.

3.3. Chemistry

Dendrimer **4**, herein adopted as nanocarrier to complex GA, and the GA-enriched dendrimer GAD (**6**) were prepared as previously described .

Concerning the novel GA delivery system (GALD, **7**), it has been achieved by dissolving dendrimer **4** in MeOH and by subjecting it to vigorously stir in the presence of a strong excess of GA (42.8 equiv.) for 48 h at room temperature in the dark (Scheme 1).

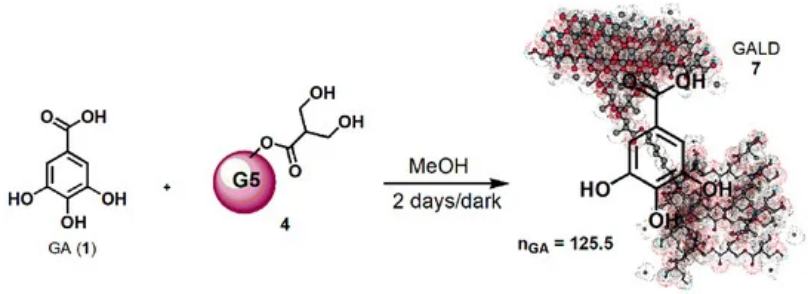

Scheme 1. Synthetic procedure for entrapping GA in dendrimer **4** (GALD **7**).

Since, as reported in the literature and Merck Index 2001, GA can be isolated by recrystallization from methanol, it was thought to purify the crude product, by removing the not entrapped free GA, through its precipitation from the final clear methanol solution. Briefly, the solution was concentrated until it became cloudy and a white solid started to separate. The precipitation was completed by placing the fine suspension at 4 °C overnight, and the obtained solid was recovered from the GALD solution by performing a centrifugation at 3500 rpm for 15 min.

GALD **7**, having the intuitive structure shown in Scheme 1, was achieved as off-white glassy solid (188.2 mg) and was stored on P_2O_5 in a dryer at r.t.

In regard to Scheme 1 and Figure 3b, the 3D structure of the dendrimer **4** was gained, using the 3D Chem Draw software (Chem 3D Pro 7.0) and the mode of representing the complex host-molecule/dendrimer herein used, was accepted as valid in a recent publication, where dendrimer **4** was employed to complex ETO [57].

3.4. Physicochemical Characterization of Dendrimer 4 and GA-Enriched Dendrimers 6 and 7

The physicochemical characterization of dendrimer **4**, not including the DLS analysis, and the complete characterization of GAD **6** have been previously reported , and the salient data are provided in SM in Figures S2,S6–S8 and Table S1. Additional experiments to determine particle size, Z-potential, and the respective PDI value of dendrimer **4**, lacking in the previous study , were performed and the results are reported in Section 3.2.9.

GALD **7** was instead qualitatively characterized, by performing the colorimetric $FeCl_3$ test for detection of phenol's presence and by Fourier Transform Infrared (FTIR) spectroscopy.

Data obtained from FTIR spectroscopy were also handled by performing Principal Component Analysis (PCA). Finally, Nuclear Magnetic Resonance (NMR) and UV–Vis analysis were carried out. UV–Vis spectrophotometric analysis associated to the Folin–Ciocalteu method was selected to evaluate the GA concentration in GALD **7** and to determine the drug loading (DL%) and the entrapment efficiency (EE%) of GALD.

In addition, UV–Vis analysis was used to investigate the GA release profile while GALD's particles were examined by Dynamic Light Scattering (DLS) analysis.

3.5. Colorimetric $FeCl_3$ Essay

To confirm the success of the complexation reaction, the $FeCl_3$ test for the detection of phenols was performed by comparing the coloration obtained on an ethanol solution of GALD (Figure S16a, Section S4 in SM) with that of a GA ethanol solution.

As shown in Figure S16b (Section S4 in SM), the strong dark blue color of the GALD solution was completely analogous to that found in the GA solution.

3.6. FTIR Characterization

An exemplificative copy of the FTIR spectrum of GALD is shown in SM Figure S17 (Section S4).

The FTIR spectra of dendrimer **4** and GA were acquired in the same conditions, for allowing the comparison between the spectra of the original components (**4** and GA) and that one of the complex (GALD). Copies of these spectra are available in SM in Figure S3 (Section S1) and Figure S13 (Section S3). FTIR analysis confirmed the success of the reaction of complexation of GA with dendrimer **4**.

In the FTIR spectrum of GA herein acquired, available in SM in Figure S13, Section S3, bands detected at 3496 and 3228 cm^{-1} (OH groups), at 3061 cm^{-1} (stretching of C–H in aromatics), at 1688 cm^{-1} (conjugated carboxyl absorption), and at 1610 cm^{-1} (C=C stretching) were considered as significant.

As shown in Figure 4 in the FTIR spectrum of GALD **7**, several bands belonging to GA and not observable in the spectrum of **4** are instead well visible, thus confirming the presence of GA in the cavities of hosting dendrimer **4**.

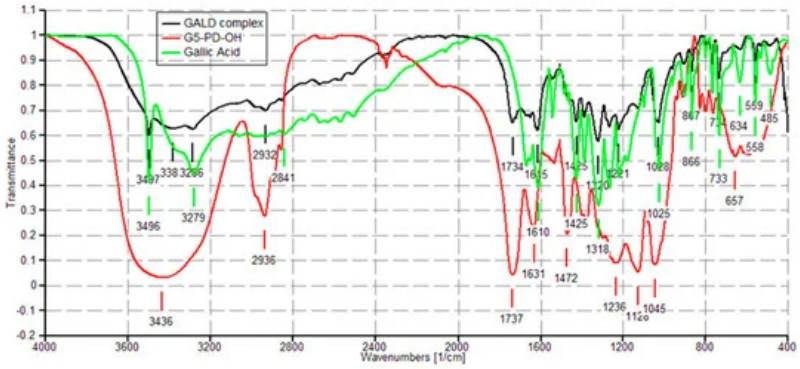

Figure 4. FTIR spectra of dendrimer **4** (red), GA (green) and GALD **7** (black).

3.7. NMR Characterization

The successful complexation of GA with dendrimer **4** was further validated by ^1H NMR spectroscopy. Since GA is a tetra-substituted phenyl derivative, in the ^1H NMR spectrum, it presents a single signal in the aromatic protons zone (7–8 ppm) belonging to the two equivalent protons in *ortho* position to the carboxyl group. Differently, dendrimer **4**, adopted to entrap GA, does not have signals in this region of the spectrum because it does not encompass aromatic rings in its structure, as obserbable in SM in Figure S4. The ^1H NMR spectrum of GALD **7** (Figure 5) presents both signals in the region 0–5 ppm, corresponding to the signals belonging to dendrimer **4** and a singlet signal at 7.15 ppm, matching the signal belonging to GA.

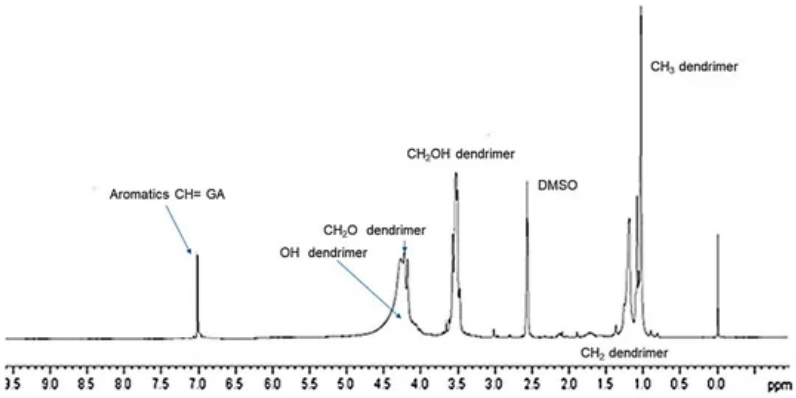

Figure 5. ^{1}H NMR (DMSO-*d6*, 300 MHz) spectrum of GALD **7**.

3.8. PCA on FTIR Spectral Data

Concerning the FTIR prediction of chemical composition of GA-enriched formulation **7**, more reliable information was achieved, by performing the PCA on data from FTIR spectra of dendrimer **4**, GA and GALD.

Briefly, PCA is able to evidence similarities or differences among the samples under study by clustering or separating them within a square of two components identified for being Information carried out by PCs is expressed in terms of percentage of explained variance. By definition, PC1 has the largest percent explained variance, followed by PC2, PC3, etc. .

In this regard, the data of nine spectra obtained by the FTIR analysis made in triplicate on dendrimer **4**, GALD **7**, and GA, were organized in a large matrix of variables, which were processed by PCA.

The results are reported as bi-plot in SM in Figure S21 (Section S6). The wanted information was unequivocally observable on PC2.

In this regard, by observing the relative positions of dendrimer **4**, GALD **7** and GA **1** on PC2, it appears that **7** is located in the first left square as GA, while the empty dendrimer **4** is located in a different square. Consequently, GALD, in terms of both location in PCA results and chemical composition, outcomes much closer to GA rather than to dendrimer **4**, suggesting that in the chemical structure of GALD **7** there is an unequivocal contribution of GA. By extrapolating the vectors up to intercept the PC2 axis, the GA loading can be estimated around 69%, i.e., higher than the expected 50%. The so high DL%, mathematically not allowed by the amounts of material employed in the complexation reaction, was confirmed by UV determination and relative explanations are discussed in the relative section.

3.9. UV–Vis Spectrophotometric Analysis of GALD

The presence of GA in GALD formulation was confirmed also by UV–Vis spectrophotometric analysis. The UV–Vis spectrum of free GA in methanol shows absorbance maxima at λ = 218 and 273 nm (Figure 6, yellow plot), while the UV–Vis spectrum of empty dendrimer **4** complexing GA, in methanol, shows no peck of absorbance in the λ range considered (not presented results).

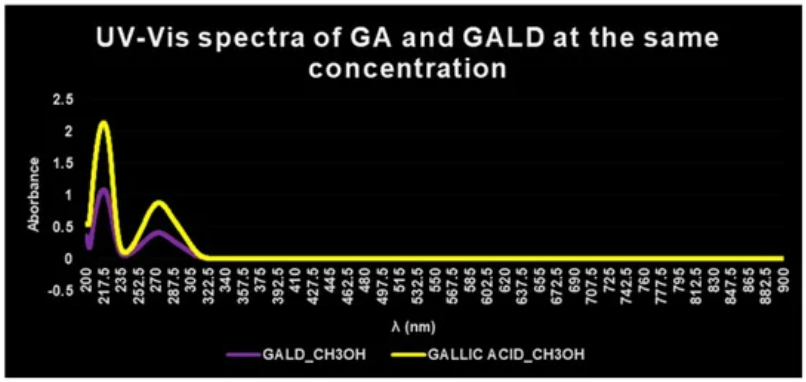

Figure 6. UV–Vis spectra of GALD **7** (violet plot) and GA (yellow plot) in methanol solution and equal concentrations.

The UV–Vis spectrum of GALD, acquired in the same solvent and at the same concentration, after dissolution and release of GA from the dendrimer scaffold, showed two absorption peaks, obviously less intense, at the same λ = 218 and 273 nm (Figure 6, violet plot).

In a study concerning GA complexes with iron[63], it was reported that, after complex formation, a bathochromic shift of the absorbance maxima of GA was observed, probably provoked by GA structural changes and/or by partial oxidation of GA caused by iron action.

Since in this case, after complex formation between GA and dendrimer **4**, no bathochromic shift in λ_{max} values was observed, it can be asserted that no structural change or oxidation processes have been occurred.

3.10. GA Content Determination

For the estimation of polyphenols such as GA, the most reported method is the well-known colorimetric Folin–Ciocalteu method based on the UV determination of the colored compounds deriving from oxidation of phenols, by the aqueous solution of phosphomolybdate and phosphotungstate (Folin–Ciocalteu reagent).

Drug Loading (DL%) was found to be 74.1% w/w.

Once known DL%, it was possible to compute both the Molecular Weight (MW) and the Encapsulation Efficiency (EE%) of GALD.

Both EE%, DL% and estimated MW of GALD resulted very high and according to what is reported , a high MW characteristically extends retention time in systemic circle and affects positively the bio-efficiency of delivering nanodevices.

3.11. In Vitro GA Release Profile from GALD

The in vitro release profile of GA from GALD **7** NPs into phosphate buffer saline solution at 37 °C and pH 7.4, mimicking human blood conditions, evaluated also to predict the GALD in vivo stability and its half-life, in reported Figure 7 as Cumulative GA release percentage in function of time. No action to stabilize GALD **7** or to influence GA release, as well as the polyester construction of dendrimer degradation, was performed.

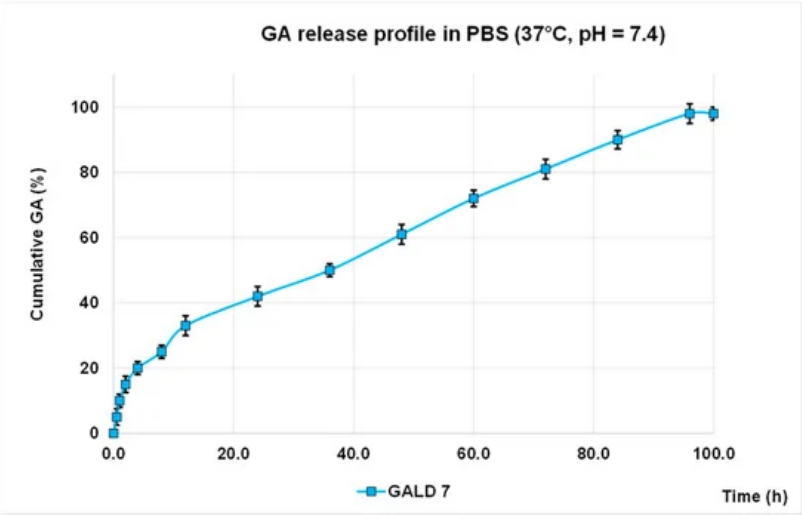

Figure 7. GA release profile in PBS, at 37 °C and pH = 7.4 expressed as cumulative percentage of release

As shown in Figure 8, an initial slight burst release of GA can be observed and only 42% of GA was released in 24 h.

The significantly softened burst release asserts a higher stability of GALD if compared to other reported cases[64][65][66] and this is a great improvement, in terms of minor systemic toxicity, over most micellar carriers, such as PEGylated PLGA-based NPs that generally have a high initial drug release [65][66].

The secondary slow and protracted release phase observed for GALD can be explained hypothesizing a degradation-controlled release and a slow degradation rate of the polyester-based scaffold of the dendrimer carrier at pH = 7.4 and at 37 °C, as reported [67].

The rather total GA release (98%) achieved suggests a complete disintegration of the carrier into small monomer compounds as previously described [67], whcih can more readily be removed from the body, allowing to minimize long-term side effects.

Finally, the initial faster release of GA, followed by a secondary slow and protracted release phase support the above-postulated presence of a part of GA associated at the surface and another part included inside of dendrimer.

3.12. Kinetics Release of GA from GALD Nanocomposite

The kinetic release of GA from the GALD nanocomposite was fitted using a number of different kinetic models, such as zero-order, first-order, Higuchi, Hixoson–Crowel, and Korsmeyer–Peppas models (Figure 8).

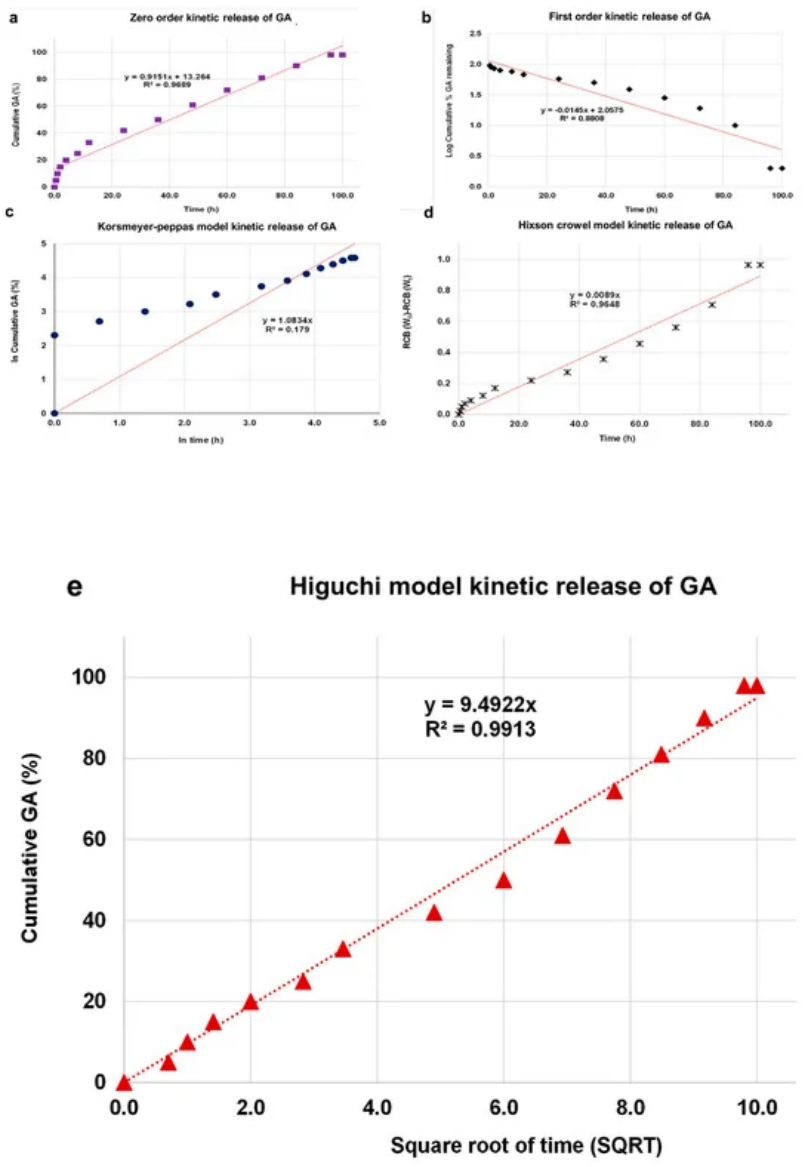

Figure 8. Fitting the data of GA release from GALD nanocomposite at pH 7.4 for kinetic models: (**a**) zero-order model; (**b**) first-order model; (**c**) Korsmeyer–Peppas model; (**d**) Hixson–Crowel model and (**e**) Higuchi model.

The results in Figure 8 establish that the release of GA from GALD **7** fits the Higuchi kinetic Model (Figure 9e).

3.13. Particle Size, Z-Potential and PDI of Dendrimer 4 and GALD

Particle sizes of dendrimer **4** and GALD were determined by DLS analysis and were expressed as Z-AVE size (nm).

Dendrimer **4** particles showed an average size of 45 nm with a satisfying PDI of 0.2, which does not denote possible formation of aggregates, confirmed by a sufficiently high Z-potential negative, assuring stability for dendrimer **4** aqueous solutions. On the other hand, NPs bearing too high surface charges, either positive or negative, attract easier macrophages.

Consequently, a Z-potential around 20 mV, as in the present case, may be promising for avoiding opsonins adsorption and subsequent clearance from the body by phagocytic cells. In addition, a Z-potential negative, probably due to the preferential absorption of hydroxyl ions on the uncharged surface of the dendrimer, hampers the binding with plasma proteins, which in turn may impede or reduce cellular up-take.

Differently, GALD particles showed an average size of 350 nm, i.e. a dimension superior to the reported optimal value of 100 nm and uncommon for dendrimers of similar generation, but in strong accordance to particle size of GAD, observable in SM in Figure S2.

As previously reported for GAD , such phenomenon is attributable to the possibility for dendrimers to form dendrimer multi-molecular assemblies, known as megamers, which are typically characterized by similar dimensions [68]. The formation of stable megamers can be intentionally provoked by introducing cross-linking agents during the dendrimer synthesis.

Otherwise, reversible megamerization can occur because of the spontaneous assemblies of dendrimer molecules into supramolecular assemblages.

In the present case, such assembly process may have been reasonably favored by the several hydroxyl groups, of both GA units and the dendrimer scaffold, which can establish many hydrogen bonds between the unimolecular dendrimer molecules, thus giving rise to dendrimers aggregates.

However, as observable in SM in Figure S27 (Section S8), particles with smaller dimensions of 119 nm, which matches the ideal value of 100 nm, are detectable.

In this regard, GALD nanoformulation, thanks to the physical properties deriving from its particles size, could possess a unique biologic potential for biomedical applications. As reported in, drug delivering devices of such dimensions represent attractive systems for treatment of cancer and heart and lung, blood, inflammatory, and infectious diseases, including central nervous system disorders. As expected, the polydispersion index (PDI) value was rather high (0.7), thus confirming the presence of particles of different sizes (100–400 nm) in water solution. Differently, the value of the zeta potential (−29 mV) was higher than expected and indicated a certain stability of GALD solutions.

It is consequently conceivable that in vivo this harmonic balance will also allow avoiding a massive phagocytic response of macrophage cells. Finally, since high positive Z-potential values are correlated to high cytotoxicity and cells internalization, while negative values allow less damage for the physiological membranes, the negative Z-potential value of −29.2 mV ± SD suggests low systemic toxicity and low cytotoxicity on health cells.

In addition, although NPs with positive Z-potential are commonly promptly absorbed on cells surface by electrostatic interactions, and are internalized more easily than ones with negative Z-potential, positive Z-potentials also favor the adsorption of negative albumin that, therefore, hampers a subsequent interaction with cell membrane and internalization.

In this regard, it was found that NPs with negative Z-potential, able to repel serum proteins, was favorable for the nanoparticles uptake in tumor cells.

3.14. Evaluation of GALD Solubility

GALD **7** gave clear and stable solutions in water at concentration of 126 mg/mL. By considering that GA DL% was 74.1%, the exact amount of GA that was possible to dissolve in water through the dissolution of GALD was 93.4mg/mL. Interestingly, the solubility of GA in water, which is a biocompatible solvent for drug administration, was improved by 6.1–8.5 times.

4. Bioactivity Results

4.1. ETOD Revealed a Synergistic Cytotoxic Effect Exerted by Dendrimer 4 *per se* and by the

Complexed ETO Slowly Released over Time

HTLA-230 NB cells were treated with 1.25 μM ETO, ETOD (in a dose capable of providing 1.25 μM ETO), and dendrimer **4** (at the same dose of that contained in the administered ETOD) for 48 and 72 h, and the effect of all treatments on NB cell viability was investigated. After 48 h of exposure to ETO, dendrimer **4**, or ETOD, the effects were comparable, since all single treatments reduced NB cell viability by 40–45%. Interestingly, comparing the effects induced by the 72 h treatment, ETOD was able to significantly reduce cell viability by 65% in respect to untreated cells and by 30% in respect to ETO-treated cells (Figure 9).

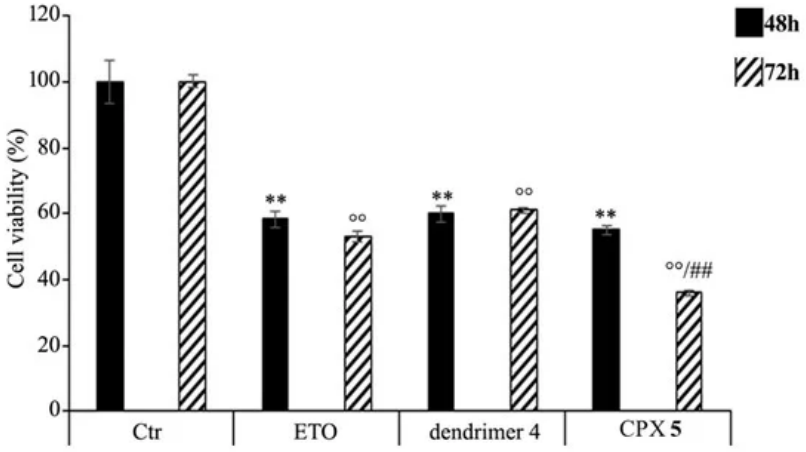

Figure 9. Cell viability was evaluated by CellTiter 96® AQueous One Solution Cell Proliferation Assay in NB cells exposed to ETO, ETOD and dendrimer **4** for 48 and 72 h. Histograms summarize quantitative data of the means ± S.E.M. of three independent experiments. ** $p < 0.01$ vs. Ctr cells (48 h); °° $p < 0.01$ vs. Ctr cells (72 h); ## $p < 0.01$ vs. ETO-treated cells (72 h).

These results demonstrate that the ETO entrapment in dendrimer **4**, although with a delayed effect, increases the cytotoxicity of the drug, and this effect is probably the result of two mechanisms that act synergistically. On one hand, ETOD guarantees a slow and protracted release of ETO over time, whereas, on the other hand, it adds a further cytotoxic effect associated to host dendrimer (**4**) to that of the delivered ETO. In our experimental model, ETOD appeared to significantly increase the cytotoxic effect of an ETO dose comparable to that commonly used to treat NB patients.

4.2. ETOD Potentiates the Cytotoxic Action of ETO by Increasing Reactive Oxygen Species (ROS) Production

As shown in Figure 10, ETOD treatment increased the production of ROS in a time-dependent manner. In particular, compared to control cells, ROS levels were increased by 70% and 190% after 48 and 72 h, respectively, while the treatment with free ETO or dendrimer **4** stimulated ROS production by 60% and 80% after 48 and 72 h (Figure 10). To our knowledge, ETO is well known to exert its cytotoxic action by increasing ROS production, while a pro-oxidant effect of nanoparticles was reported only for polyamidoamine dendrimers (PAMAMs). Our present data shows that dendrimer **4**, which was able per se to increase ROS production, when included in the formation of ETOD, markedly enhanced the pro-oxidant action of ETO, thus creating conditions of oxidative stress capable of triggering cell death (Figure 10).

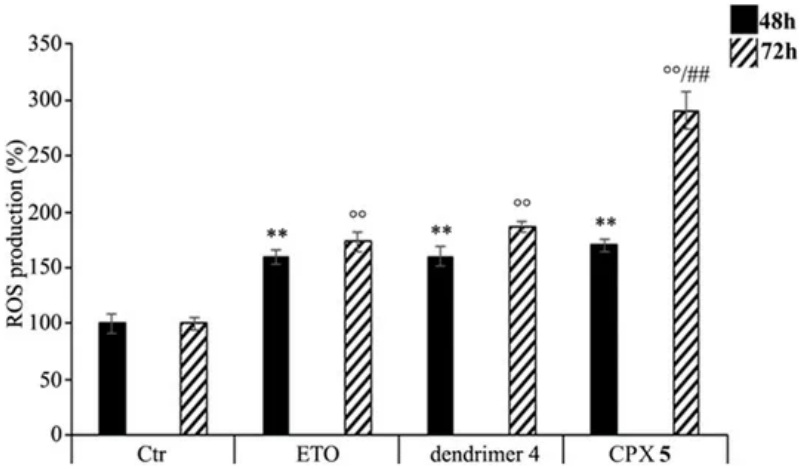

Figure 10. Reactive oxygen species (ROS) generation was analyzed in neuroblastoma (NB) cells exposed to ETO, ETOD and dendrimer **4** for 48 and 72 h. Histograms summarize quantitative data of the means ± SEM. of three independent experiments. ** $p < 0.01$ vs. Ctr cells (48 h); °° $p < 0.01$ vs. Ctr cells (72 h); ## $p < 0.01$ vs. ETO-treated cells (72 h).

4.3. Time-Course and Dose-Dependent Experiments on GA

Since it was the first time that GA was considered as alternative possible compound to treat human NB, time-course dose-dependent experiments were performed to evaluate its effects on NB cells viability and intracellular ROS induction.

The activity of free GA, both on ROS production and on NB cells viability, in function of GA concentrations (10–150 μM) and time of cells exposure (48 and 72 h) were assayed both on HTLA-230 and on HTLA-ER NB cells [12].

The findings asserted that a significant improvement of ROS production was observable at concentrations of 100 and 150 μM for HTLA-230 and HTLA-ER cells, respectively, after 48 h, and at concentrations of 75 and 100 μM for HTLA-230 and HTLA-ER, respectively, after 72 h , thus confirming a time dependent pro-oxidant action.

Accordingly, a significant reduction in cells viability was observed at concentrations of 100 and 150 μM for HTLA-230 and HTLA-ER cells, respectively, after 48 h, and of 75 and 100 μM for HTLA-230 and HTLA-ER, respectively, after 72 h.

Both the GA-induced ROS production and cytotoxicity were more marked in the cells sensitive to ETO than in the resistant ones, which have developed enhanced antioxidant defenses [12].

These findings confirm that also GA cytotoxic activity depends on length of cell exposure and suggest a cause–effect relationship between ROS production and cytotoxicity.

In fact, this correlation, extensively reported for phytochemicals such as GA [68], was further confirmed by the exact overlap of the active concentrations of GA able to cause both a significant increase in ROS and a significant decrease in cell viability at 48 and 72 h.

In addition, as reported for many other kinds of tumors [69], these findings confirmed that, also on NB cells, GA exerts a ROS-mediated cytotoxic anticancer activity at high doses, while it loses its pro-oxidant properties at low doses [68].

At doses lower than 75 μM, GA did not influence significantly ROS production or viability of both NB cells populations, further confirming that ROS production and the cytotoxic action are correlated by a cause–effect relationship.

4.4. Evaluation of Cytotoxic Action of GAD, GALD, GA and Empty Dendrimer 4 on Human Neuroblastoma Cells

HTLA-230 and HTLA-ER NB cells [12] were treated with dendrimer **4** at the reported active concentration of 0.169 μM , GALD at a concentration capable of providing 0.169 μM dendrimer **4**, and GA at the concentration (21.20 μM) provided by the amount of GALD used. Then, to get the same concentration of GA provided by GALD, since GAD contains 64 GA units, its concentration was computed by dividing by 64 the concentration of 21.20 μM, which was 0.3313 μM. The cells were exposed to dendrimer **4**, GALD, GAD, and GA for 48 and 72 h and the effect of all treatments on NB cell viability was investigated. The results asserted that 48 h of exposure to dendrimer **4** reduced HTLA-230 and HTLA-ER cell viability by 40% and 20%, respectively. Interestingly, comparing the effects induced by the 72-h treatment, dendrimer **4** further reduced by 5% the cell viability of both cell populations. As expected, free GA did not affect cell viability after 48 and 72 h, due to the low dose employed, in both cells populations.

Unexpectedly, at the used concentrations providing the amount of dendrimer **4** active when administered alone, the exposure to GAD or GALD did not affect cell viability after 48 and 72 h in both cell populations, highlighting instead that the presence of GA in the GAD and GALD formulations totally prevented the cytotoxic action of dendrimer **4**.

These results demonstrate that dendrimer **4**, in addition to inducing death in NB cells sensitive to ETO , is able to exert cytotoxic effects also in chemoresistant NB cells population.

In this regard, dendrimer **4** represents a nanodevice suggestable either as a promising novel therapeutic molecule, able to induce death, in both sensitive and resistant NB cells at low dose, and/or as a carrier for chemotherapeutic drugs, for realizing synergistic therapies and reducing drugs dosage.

As a confirmation for the feasibility of this strategy for treating NB, recently it has been demonstrated that the encapsulation of ETO into the dendrimer **4** enhances ETO activity in a time-dependent way and facilitates its protracted release .

The results herein obtained in GA-treated cells at concentrations sub-active of GA confirm those obtained in the time-course and dose-dependent experiments, which show that, as reported previously [23],[24], GA cytotoxic action is dose dependent and is performed only at high dosage, similar to many natural antioxidant–pro-oxidant compounds .

Although GA ROS-mediated cytotoxicity at low dose was not improved, by reformulating GA in NPs interesting findings and an unexpected goal were achieved.

Through the reformulation of low concentrations of GA in NPs, by using bioactive concentrations of dendrimer **4** and two different synthetic strategies, two nanosized forms of GA were achieved that, surprisingly, proved to exert such remarkable antioxidant effects as to be able to completely abolish the pro-oxidant and cytotoxic activities of the dendrimer.

4.5. The Presence of GA Nullifies the Pro-Oxidant Action of Dendrimer 4 in NB Cells Exposed to GAD and GALD

Dendrimer **4** proved to be able to increase ROS production in both cell populations, although this effect was more evident in HTLA-230 than in HTLA-ER cells. On the contrary, in both cell populations, the exposure to free GA did not change ROS production at 48 or 72 h, as in the case of cells viability, due to the low dose employed. Moreover, in these cell populations, a slight potentiation of antioxidant power of GA was observed for both GAD and GALD. The strong antioxidant activity of GA, when reformulated in NPs, was distinctly highlighted by the finding that it was able to nullify ROS overproduction induced by the dendrimer **4** in both cell populations, at low dose and either at 48 and 72 h.

Returning to dendrimer **4**, thanks to its pro-oxidant activity, it was able to create a condition of OS responsible for triggering NB cell death also in chemoresistant populations.

Since NB cells, and in particular chemoresistant ones, have been demonstrated to activate antioxidant responses [12][13], the induction of OS could be efficiently employed to sensitize cancer cells to pro-oxidant cytotoxic action of chemotherapeutic drugs. In this regard, we have demonstrated that the combination of ETO with dendrimer **4** by increasing the pro-oxidant action of ETO is able to sensitize not resistant NB cells to the drug .

This strategy could become useful in vivo to enhance sensitivity of tumors to antineoplastic agents by lowering drug’s cytotoxic doses and therefore their systemic toxicity.

5. Conclusions

The interesting results from the present study suggest that novel promising strategies can be developed for treating cancer, by applying nanotechnology and natural compounds. In regard to NB, to date not yet faced with GA, GA was able to exert a ROS-mediated cytotoxic action, both on sensitive and on chemoresistant NB cells, only at high concentrations (75–150 µM), and it was considered safe. Interestingly, the nanoengineered dendrimer **4**, previously found to possess a ROS-mediated cytotoxic activity on sensitive NB cells, in this study showed to be able to chemosensitize also NB cells resistant to ETO at a concentration almost 100-fold lower than that of GA.

In this regard, dendrimer **4** nanodevice is advisable, either as a promising novel therapeutic drug effective also on cells resilient to available drugs or as an advantageous and synergistic carrier for chemotherapeutic drugs, thus allowing reducing their dosage, systemic toxicity, and side effects. Moreover, dendrimer **4** represents for researchers a useful template molecule for the development of a variety of analogous dendrimer devices endowed with cytotoxic activity against NB cells.

Differently, the GA-enriched dendrimers GAD and GALD, administered at concentrations providing bioactive amounts of dendrimer **4** and concentrations of GA not able to induce ROS-mediated cells death, proved to be ineffective against NB.

Synthetizing and assaying GAD and GALD was not fruitless, because it allowed observing that the presence of GA, in GAD and GALD formulations, slowed down (HTLA-ER cells) or nullified (HTLA230) the pro-oxidant activity showed by dendrimer **4** when administered alone.

In NB cells, this GA behavior hindered the ROS-mediated anti-cancer effect of dendrimer **4** against NB cells, but suggests a considerable ability of GA in counteracting ROS overproduction and OS, induced by **4**, also at low doses, when resized in form of NPs.

These findings could have important clinical repercussions for two reasons. On the one hand, the results advise scientists that it is crucial to be careful to administer nanoformulated polyphenol-enriched food supplements to cancer patients treated with pro-oxidant chemotherapeutic drugs, because polyphenol NPs could invalidate their effectiveness, as GA versus dendrimer **4**.

On the other hand, the above findings evidence that, when reformulated in NPs, GA takes on the ability to inactivate compounds able to induce ROS and OS, which are the major causes of DNA damage and cancer initiation in healthy cells.

Concerning encapsulation of ETO, the drug loading was 37%, the entrapment efficiency was 89%, and the solubility of ETO in biocompatible solvents was amazingly improved (390 times in H_2O). Experiments performed to assess ETOD bioactivity on NB cells in comparison with ETO and dendrimer **4** alone demonstrated that in ETOD, the bioactive scaffold of dendrimer **4** has been found to act in synergy with the complexed ETO that was released in a protracted manner, determining a significant improvement of the cytotoxic activity of free ETO. In addition, having a high drug loading and providing the hosted ETO with a protective shell, ETOD guaranteed an improvement of the ROS-mediated cytotoxic action of ETO for a long time.

Consequently, although preliminary, our data suggests that ETOD, endowed with a considerably improved water solubility and a significant scaffold-assisted anti-cancer activity, can become a promising formulation for the protracted release of ETO in order to sensitize NB cells. The already very interesting and satisfying results obtained by combining ETO with the not functionalized dendrimer **4** could be further improved by the partially esterification of the peripheral hydroxyls of **4** with targeting molecules such as folic acid that is recognized by cancer cells for a more selective action and reduced toxicity for healthy cells.

It is clear that each of the compounds investigated in this work (GA, dendrimer **4**, GAD **6**, and GALD **7**) deserves further and more in deep investigations to clarify its mechanism of action at the molecular level. In this context, experiments on dendrimer **4**, in order to investigate the metabolic pathway responsible for ROS overproduction and NB cell death, are already underway. In addition, another polyester-based scaffold, analogous of **4** but slightly modified in the structure, is also under study, in order to find how structural modifications could influence cytotoxic activity.

In addition, thinking of a future clinical application of dendrimers, it is the duty of the authors to remember the general concern regarding the potential dangerous effects of nanomaterials on human health. In addition to existing in various sizes, shapes, and chemical compositions, NPs occur also in different degrees of agglomeration. Intracellular distribution is affected by agglomeration and agglomeration may represent a risk factor because it enables NPs to accumulate within the tissue, thus reducing clearance efficiency and improving toxicity. In this regard, knowledge regarding agglomeration-based accumulation and its relevance is still limited. The currently available in vitro literature is controversial, and findings regarding the effect of agglomeration are poor, thus it is strongly recommended to include these aspects in future investigations.

References

1. John M. Maris; Recent advances in neuroblastoma.. *New England Journal of Medicine* **2010**, *362*, 2202-11, 10.1056/NEJMra0804577.
2. Nai-Kong V. Cheung; Michael Dyer; Neuroblastoma: developmental biology, cancer genomics and immunotherapy.. *Nature Reviews Cancer* **2013**, *13*, 397-411, 10.1038/nrc3526.
3. Srishma Sridhar; Batool Al-Moallem; Hawra Kamal; Marta Terrile; Raymond L. Stallings; New Insights into the Genetics of Neuroblastoma. *Molecular Diagnosis & Therapy* **2013**, *17*, 63-69, 10.1007/s40291-013-0019-6.
4. Maris, J.M.; Hogarty, M.D.; Bagatell, R.; Cohn, S.L.; Neuroblastoma. *Lancet* **2007**, *369*, 2106–2120, https://doi.org/10.1016/S0140-6736(07)60983-0.
5. Alberto Garaventa; Roberto Luksch; Simona Biasotti; Gianluca Severi; Maria Rosa Pizzitola; Elisabetta Viscardi; Arcangelo Prete; Stefano Mastrangelo; Marta Podda; Riccardo Haupt; et al. A phase II study of topotecan with vincristine and doxorubicin in children with recurrent/refractory neuroblastoma. *Cancer* **2003**, *98*, 2488-2494, 10.1002/cncr.11797.

6. T. Simon; Alfred Längler; Urs Harnischmacher; Michael C. Frühwald; Norbert Jorch; Alexander Claviez; Frank Berthold; Barbara Hero; Topotecan, cyclophosphamide, and etoposide (TCE) in the treatment of high-risk neuroblastoma. Results of a phase-II trial. *Journal of Cancer Research and Clinical Oncology* **2007**, *133*, 653-661, 10.1007/s00432-007-0216-y.
7. T. Simon; Alfred Längler; Urs Harnischmacher; Michael C. Frühwald; Norbert Jorch; Alexander Claviez; Frank Berthold; Barbara Hero; Topotecan, cyclophosphamide, and etoposide (TCE) in the treatment of high-risk neuroblastoma. Results of a phase-II trial. *Journal of Cancer Research and Clinical Oncology* **2007**, *133*, 653-661, 10.1007/s00432-007-0216-y.
8. Riccardo Haupt; Thomas R. Fears; Ansgar Heise; Helmut Gadner; Giuseppe Lolacono; Marino De Terlizzi; Margaret A. Tucker; Risk of secondary leukemia after treatment with etoposide (VP-16) for Langerhans' cell histiocytosis in Italian and Austrian-German populations.. *International Journal of Cancer* **1997**, *71*, 9-13, 10.1002/(sici)1097-0215(19970328)71:1<9::aid-ijc3>3.0.co;2-y.
9. Haupt, R.; Fears, T.R.; Heise, A.; Gadner, H.; Loiacono, G.; De Terlizzi, M.; Tucker, M.A.; Risk of secondary leukemia after treatment with etoposide (VP-16) for Langerhans'cell histiocytosis in Italian and Austrian-German populations. *Int. J. Cancer* **1997**, *71*, 9-13, https://doi.org/10.1002/(SICI)1097-0215(19970328)71:1%3C9::AID-IJC3%3E3.0.CO;2-Y.
10. Bernardini, S.; Bellincampi, L.; Ballerini, S.; Ranalli, M.; Pastore, A.; Cortese, C.; Federici, G.; Role of GST P1-1 in mediating the effect of etoposide on human neuroblastoma cell line Sh-Sy5y. *J. Cell. Biochem.* **2002**, *86*, 340–347, https://doi.org/10.1002/jcb.10219.
11. Renata Colla; Alberto Izzotti; Chiara De Ciucis; Daniela Fenoglio; Silvia Ravera; Andrea Speciale; Roberta Ricciarelli; Anna Lisa Furfaro; Alessandra Pulliero; Mario Passalacqua; et al. Glutathione-mediated antioxidant response and aerobic metabolism: two crucial factors involved in determining the multi-drug resistance of high-risk neuroblastoma. *Oncotarget* **2016**, *7*, 70715-70737, 10.18632/oncotarget.12209.
12. Nicola Traverso; Roberta Ricciarelli; Mariapaola Nitti; Barbara Marengo; Anna Lisa Furfaro; Maria Adelaide Pronzato; Umberto Maria Marinari; Cinzia Domenicotti; Role of Glutathione in Cancer Progression and Chemoresistance. *Oxidative Medicine and Cellular Longevity* **2013**, *2013*, 1-10, 10.1155/2013/972913.
13. João Pedro Silva; O P Coutinho; Free radicals in the regulation of damage and cell death - basic mechanisms and prevention.. *Drug Discoveries & Therapeutics* **2010**, *4*, 144–167, https://www.ddtjournal.com/article/317.
14. Liu, Z.; Ren, Z.; Zhang, J.; Chuang, C.C.; Kandaswamy, E.; Zhou, T.; Zuo, L.; Role of ROS and Nutritional Antioxidants in Human Diseases. *Front. Physiol.* **2018**, *9*, 477, https://doi.org/10.3389/fphys.2018.00477.
15. Stefania D'angelo; Elisa Martino; Concetta Paola Ilisso; Maria Libera Bagarolo; Marina Porcelli; Giovanna Cacciapuoti; Pro-oxidant and pro-apoptotic activity of polyphenol extract from Annurca apple and its underlying mechanisms in human breast cancer cells. *International Journal of Oncology* **2017**, *51*, 939-948, 10.3892/ijo.2017.4088.
16. Aborehab, N.M.; Osama, N.; Effect of Gallic acid in potentiating chemotherapeutic effect of Paclitaxel in HeLa cervical cancer cells. *Cancer Cell Int.* **2019**, *19*, 154, 10.1186/s12935-019-0868-0.
17. Matija Strlic; Tanja Radovič; Jana Kolar; Boris Pihlar; Anti- and Prooxidative Properties of Gallic Acid in Fenton-Type Systems. *Journal of Agricultural and Food Chemistry* **2002**, *50*, 6313-6317, 10.1021/jf025636j.
18. Dan Li; Zuojia Liu; Wenjing Zhao; Yanli Xi; Fenglan Niu; A straightforward method to determine the cytocidal and cytopathic effects of the functional groups of gallic acid. *Process Biochemistry* **2011**, *46*, 2210-2214, 10.1016/j.procbio.2011.08.011.
19. Somayeh Hajipour; Alireza Sarkaki; Yaghoob Farbood; Akram Eidi; Pejman Mortazavi; Zohreh Valizadeh; Effect of Gallic Acid on Dementia Type of Alzheimer Disease in Rats: Electrophysiological and Histological Studies. *Basic and Clinical Neuroscience Journal* **2016**, *7*, 97-106, 10.15412/J.BCN.03070203.
20. Jadel M. Kratz; Carla Regina Andrighetti-Fröhner; Paulo César Leal; Ricardo José Nunes; Rosendo Augusto Yunes; Edward Trybala; Tomas Bergström; Célia Regina Monte Barardi; Cláudia Maria Oliveira Simões; Evaluation of anti-HSV-2 activity of gallic acid and pentyl gallate.. *Biological & Pharmaceutical Bulletin* **2008**, *31*, 903-907, 10.1248/bpb.31.903.
21. Salucci, M.; Stivala, L.A.; Maiani, G.; Bugianesi, R.; Vannini, V.; Flavonoids uptake and their effect on cell cycle of human colon adenocarcinoma cells (Caco2).. *Br. J. Cancer* **2002**, *86*, Br. J. Cancer 2002, 86, 1645–1651, doi: 10.1038/sj.bjc.6600295..
22. M. Inoue; R. Suzuki; T. Koide; N. Sakaguchi; Y. Ogihara; Y. Yabu; Antioxidant, Gallic Acid, Induces Apoptosis in HL-60RG Cells. *Biochemical and Biophysical Research Communications* **1994**, *204*, 898-904, 10.1006/bbrc.1994.2544.
23. Kawada, M.; Ohno, Y.; Ri, Y.; Ikoma, T.; Yuugetu, H.; Asai, T.; Anti-tumor effect of gallic acid on LL-2 lung cancer cells transplanted in mice.. *Anticancer Drugs* **2001**, *12*, 847–852., doi: 10.1097/00001813-200111000-00009.

24. Zahra Sourani; Batoul Pourgheysari; Pezhman Beshkar; Hedayatollah Shirzad; Moein Shirzad; Gallic Acid Inhibits Proli feration and Induces Apoptosis in Lymphoblastic Leukemia Cell Line (C121). *Iranian Journal of Medical Sciences* **1970**, *41*, 525-530, .

25. Makoto Inoue; Rie Suzuki; Nahoko Sakaguchi; Zong Li; T Takeda; Yukio Ogihara; Bao Yuan Jiang; Yingjie Chen; Select ive Induction of Cell Death in Cancer Cells by Gallic Acid.. *Biological & Pharmaceutical Bulletin* **1995**, *18*, 1526-1530, 1 0.1248/bpb.18.1526.

26. Aikebaier Maimaiti; Amier Aili; Hureshitanmu Kuerban; Xuejun Li; VDAC1 Mediated Anticancer Activity of Gallic Acid in Human Lung Adenocarcinoma A549 Cells. *Anti-Cancer Agents in Medicinal Chemistry* **2018**, *18*, 255-262, 10.2174/187 152061766617091211544 1.

27. Sibylle Madlener; Christoph Illmer; Zsuzsanna Horvath; Philipp Saiko; Annemarie Losert; Irene Herbacek; Michael Grus ch; Howard L. Elford; Georg Krupitza; Astrid Bernhaus; et al. Gallic acid inhibits ribonucleotide reductase and cyclooxyg enases in human HL-60 promyelocytic leukemia cells. *Cancer Letters* **2007**, *245*, 156-162, 10.1016/j.canlet.2006.01.00 1.

28. Nowak, R.; Olech, M.; Nowacka, N. Polyphenols in Human Health and Disease; Elsevier, Eds.; Elsevier: Amsterdam, T he Netherlands, 2014; pp. 1289–1307.

29. Bharti Badhani; Neha Sharma; Rita Kakkar; Gallic acid: a versatile antioxidant with promising therapeutic and industrial applications. *RSC Advances* **2015**, *5*, 27540-27557, 10.1039/c5ra01911g.

30. L. Li; T.B. Ng; Wei Gao; W. Li; M. Fu; S.M. Niu; L. Zhao; R.R. Chen; F. Liu; Antioxidant activity of gallic acid from rose fl owers in senescence accelerated mice. *Life Sciences* **2005**, *77*, 230-240, 10.1016/j.lfs.2004.12.024.

31. Ruixuan Wang; Lijie Ma; Dan Weng; Jiahui Yao; Xueying Liu; Faguang Jin; Gallic acid induces apoptosis and enhance s the anticancer effects of cisplatin in human small cell lung cancer H446 cell line via the ROS-dependent mitochondrial apoptotic pathway. *Oncology Reports* **2016**, *35*, 3075-3083, 10.3892/or.2016.4690.

32. Hsieh-Hsun Ho; Chi-Sen Chang; Wei-Chi Ho; Sheng-You Liao; Cheng-Hsun Wu; Chau-Jong Wang; Anti-metastasis eff ects of gallic acid on gastric cancer cells involves inhibition of NF-κB activity and downregulation of PI3K/AKT/small GT Pase signals. *Food and Chemical Toxicology* **2010**, *48*, 2508-2516, 10.1016/j.fct.2010.06.024.

33. Jeng-Dong Hsu; Shao-Hsuan Kao; Ting-Tsz Ou; Yu-Jen Chen; Yi-Ju Li; Chau-Jong Wang; Gallic Acid Induces G2/M Ph ase Arrest of Breast Cancer Cell MCF-7 through Stabilization of p27Kip1Attributed to Disruption of p27Kip1/Skp2 Comp lex. *Journal of Agricultural and Food Chemistry* **2011**, *59*, 1996-2003, 10.1021/jf103656v.

34. Li-Li Lu; Xiu-Yang Lu; Solubilities of Gallic Acid and Its Esters in Water. *Journal of Chemical & Engineering Data* **2007**, *52*, 37-39, 10.1021/je0601661.

35. Padilla De Jesus, O.L.; Ihre, H.R.; Gagne, L.; Frechet, J.M.J.; Szoka, F.C.; Polyester dendritic systems for drug delivery applications: In vitro and in vivo evaluation.. *Bioconjug. Chem.* **2002**, *13*, 453–461, https://doi.org/10.1021/bc010103m.

36. Silvana Alfei; Federica Turrini; Silvia Catena; Paola Zunin; Brunella Parodi; Guendalina Zuccari; Anna Pittaluga; Raffael la Boggia; Preparation of ellagic acid micro and nano formulations with amazingly increased water solubility by its entra pment in pectin or non-PAMAM dendrimers suitable for clinical applications. *New Journal of Chemistry* **2019**, *43*, 2438-2448, 10.1039/c8nj05657a.

37. Cameron C Lee; John A Mackay; Jean M.J. Fréchet; Francis C Szoka; Designing dendrimers for biological application s. *Nature Biotechnology* **2005**, *23*, 1517-1526, 10.1038/nbt1171.

38. Rami Hourani; Ashok Kakkar; Advances in the Elegance of Chemistry in Designing Dendrimers. *Macromolecular Rapid Communications* **2010**, *31*, 947-974, 10.1002/marc.200900712.

39. Silvana Alfei; Gaby Brice Taptue; Silvia Catena; Angela Bisio; Synthesis of Water-soluble, Polyester-based Dendrimer Prodrugs for Exploiting Therapeutic Properties of Two Triterpenoid Acids. *Chinese Journal of Polymer Science* **2018**, *3 6*, 999-1010, 10.1007/s10118-018-2124-9.

40. Silvana Alfei; Silvia Catena; Marco Ponassi; Camillo Rosano; Vittoria Zoppi; Andrea Spallarossa; Hydrophilic and amph iphilic water-soluble dendrimer prodrugs suitable for parenteral administration of a non-soluble non-nucleoside HIV-1 re verse transcriptase inhibitor thiocarbamate derivative. *European Journal of Pharmaceutical Sciences* **2018**, *124*, 153-1 64, 10.1016/j.ejps.2018.08.036.

41. Keerti Jain; Prashant Kesharwani; Umesh Gupta; Narendra K. Jain; Dendrimer toxicity: Let's meet the challenge. *Intern ational Journal of Pharmaceutics* **2010**, *394*, 122-142, 10.1016/j.ijpharm.2010.04.027.

42. Jin-Seong Lee; June Huh; Cheol-Hee Ahn; Minhyung Lee; Tae Gwan Park; Synthesis of Novel Biodegradable Cationic Dendrimers. *Macromolecular Rapid Communications* **2006**, *27*, 1608-1614, 10.1002/marc.200600393.

43. Ma, X.; Tang, J.; Shen, Y.; Fan, M.; Tang, H.; Radosz, M; Facile synthesis of polyester dendrimers from sequential click coupling of asymmetrical monomers.. *J. Am. Chem. Soc.* **2009**, *131*, 14795–14803. , doi: 10.1021/ja9037406..

44. Sharma, A.; Gautam, S.P.; Gupta, A.K.; Surface modified dendrimers: Synthesis and characterization for cancer targete d drug delivery.. *Bioorg. Med. Chem.* **2011**, *19*, 3341–3346, https://doi.org/10.1016/j.bmc.2011.04.046.

45. Barbara Klajnert-Maculewicz; Maria Bryszewska; Interactions between PAMAM dendrimers and gallic acid molecules s tudied by spectrofluorimetric methods. *Bioelectrochemistry* **2007**, *70*, 50-52, 10.1016/j.bioelechem.2006.03.027.

46. Liron Bitan-Cherbakovsky; Abraham Aserin; Nissim Garti; Structural characterization of lyotropic liquid crystals containi ng a dendrimer for solubilization and release of gallic acid. *Colloids and Surfaces B: Biointerfaces* **2013**, *112*, 87-95, 1 0.1016/j.colsurfb.2013.06.051.

47. Sandra P. Amaral; Marcos Fernandez-Villamarin; Juan Correa; Ricardo Riguera; Eduardo Fernandez-Megia; Efficient Multigram Synthesis of the Repeating Unit of Gallic Acid-Triethylene Glycol Dendrimers. *Organic Letters* **2011**, *13*, 452 2-4525, 10.1021/ol201677k.

48. De la Fuente, M.; Raviña, M.; Sousa-Herves, A.; Correa, J.; Riguera, R.; Fernandez-Megia, E.; Sánchez, A.; Alonso, M. J.; Exploring the efficiency of gallic acid-based dendrimers and their block copolymers with PEG as gene carriers. *Nano medicine* **2012**, *7*, 1667–1681, https://doi.org/10.2217/nnm.12.51.

49. Renu Singh Dhanikula; Patrice Hildgen; Synthesis and Evaluation of Novel Dendrimers with a Hydrophilic Interior as N anocarriers for Drug Delivery. *Bioconjugate Chemistry* **2006**, *17*, 29-41, 10.1021/bc050184c.

50. Henrik Ihre; Anders Hult; Jean M.J. Fréchet; Ivan Gitsov; Double-Stage Convergent Approach for the Synthesis of Func tionalized Dendritic Aliphatic Polyesters Based on 2,2-Bis(hydroxymethyl)propionic Acid. *Macromolecules* **1998**, *31*, 40 61-4068, 10.1021/ma9718762.

51. Ihre, H.; Hult, A.; Fréchet, J.M.J.; Gitsov, I. Double-Stage Convergent Approach for the Synthesis of Functionalized Den dritic Aliphatic Polyesters Based on 2,2-Bis(hydroxymethyl)propionic Acid. Macromolecules 1998, 31, 4061–4068. [Goo gle Scholar] [CrossRef]

52. Alfei, S.; Castellaro, S.; Taptue, G.B. Synthesis and NMR characterization of dendrimers based on 2, 2-bis-(hydroxymet hyl)-propanoic acid (bis-HMPA) containing peripheral amino acid residues for gene transfection. Org. Commun. 2017, 1 0, 144–147. [Google Scholar] [CrossRef]

53. Alfei, S.; Castellaro, S. Synthesis and characterization of polyester-based dendrimers containing peripheral arginine or mixed amino acids as potential vectors for gene and drug delivery. Macromol. Res. 2017, 25, 1172–1186. [Google Sch olar] [CrossRef]

54. Alfei, S.; Catena, S.; Turrini, F. Biodegradable and biocompatible spherical dendrimer nanoparticles with a gallic acid sh ell and a double-acting strong antioxidant activity as potential device to fight diseases from “oxidative stress”. Drug Deli v. Transl. Res. 2020, 10, 259–270. [Google Scholar] [CrossRef] [PubMed]

55. Alfei, S.; Oliveri, P.; Malegori, C. Assessment of the Efficiency of a Nanospherical Gallic Acid Dendrimer for Long-Term Preservation of Essential Oils: An Integrated Chemometric-Assisted FTIR Study. ChemistrySelect 2019, 4, 8891–8901. [Google Scholar] [CrossRef]

56. Alfei, S.; Signorello, M.G.; Schito, A.M.; Catena, S.; Turrini, F. Reshaped as polyester-based nanoparticles, gallic acid i nhibits platelet aggregation, reactive oxygen species production and multi-resistant Gram-positive bacteria with an effici ency never obtained. Nanoscale Adv. 2019, 1, 4148–4157. [Google Scholar] [CrossRef]

57. Alfei, S.; Marengo, B.; Domenicotti, C. Polyester-Based Dendrimer Nanoparticles Combined with Etoposide Have an I mproved Cytotoxic and Pro-Oxidant Effect on Human Neuroblastoma Cells. Antioxidants 2020, 9, 50. [Google Scholar] [CrossRef] [PubMed]

58. Medina, S.H.; El-Sayed, M.E.H. Dendrimers as carriers for delivery of chemotherapeutic agents. Chem. Rev. 2009, 10 9, 3141–3157. [Google Scholar] [CrossRef] [PubMed]

59. Alfei, S.; Catena, S. Synthesis and characterization of fourth generation polyester-based dendrimers with cationic amin o acids-modified crown as promising water soluble biomedical devices. Polym. Adv. Technol. 2018, 29, 2735–2749. [Go ogle Scholar] [CrossRef]

60. Choudhary, S.; Gupta, L.; Rani, S.; Dave, K.; Gupta, U. Impact of Dendrimers on Solubility of Hydrophobic Drug Molec ules. Front. Pharmacol. 2017, 16, e261. [Google Scholar] [CrossRef] [PubMed]

61. Kaminskas, L.M.; Boyd, B.J.; Porter, C.J.H. Dendrimer pharmacokinetics: The effect of size, structure and surface char acteristics on ADME properties. Nanomedicine 2011, 6, 1063–1084. [Google Scholar] [CrossRef]

62. Marengo, B.; Monti, P.; Miele, M.; Menichini, P.; Ottaggio, L.; Foggetti, G.; Pulliero, A.; Izzotti, A.; Speciale, A.;Garbarin o, O.; et al. Etoposide-resistance in a neuroblastoma model cell line is associated with 13q14.3 mono-allelic deletion an d miRNA-15a/16-1 down-regulation. Sci. Rep. 2018, 8, 13762. [CrossRef] [PubMed]

63. Jancovivova, V.; Ceppan, M.; Havlinova, B.; Rehakova, M.; Jakubikova, Z. Interactions in iron gall inks. Chem. Pap. 20 07, 61, 391–397. [Google Scholar] [CrossRef]

64. Huang, X.; Brazel, C.S. On the importance and mechanisms of burst release in matrix-controlled drug delivery system s. J. Control Release 2001, 73, 121–136. [Google Scholar] [CrossRef]
65. Danhier, F.; Lecouturier, N.; Vroman, B.; Jerome, C.; Marchand-Brynaert, J.; Feron, O.; Preat, V. Paclitaxel-loaded PEG ylated PLGA-based nanoparticles: In vitro and in vivo evaluation. J. Control Release 2009, 133, 11–17. [Google Schola r] [CrossRef]
66. Ma, X.; Zhou, Z.; Jin, E.; Sun, Q.; Zhang, B.; Tang, J.; Shen, Y. Facile synthesis of polyester dendrimers as drug deliver y carriers. Macromolecules 2013, 46, 37–42. [Google Scholar] [CrossRef]
67. Feliu, N.; Walter, W.V.; Montañez, M.I.; Kunzmann, A.; Hult, A.; Nyström, A.; Malkoch, M.; Fadeelet, B. Stability and bio compatibility of a library of polyester dendrimers in comparison to polyamidoamine dendrimers. Biomaterials 2012, 33, 1970–1981. [Google Scholar] [CrossRef]
68. Manjappa, K.; Narayanaswamy, J. Thiol-Disulfide Interchange Mediated Reversible Dendritic Megamer Formation and Dissociation. Macromolecules 2009, 42, 7353–7359. [Google Scholar] [CrossRef]
69. Gao, J.; Hu, J.; Hu, D.; Yang, X. A Role of Gallic Acid in Oxidative Damage Diseases: A Comprehensive Review. Nat. P rod. Commun. 2019, 14, 1–9. [Google Scholar] [CrossRef]
